

# Midbrain dopamine neurons encode decisions for future action

Genela Morris<sup>1,2</sup>, Alon Nevet<sup>2</sup>, David Arkadir<sup>2</sup>, Eilon Vaadia<sup>1,2</sup> & Hagai Bergman<sup>1,2</sup>

**Current models of the basal ganglia and dopamine neurons emphasize their role in reinforcement learning. However, the role of dopamine neurons in decision making is still unclear. We recorded from dopamine neurons in monkeys engaged in two types of trial: reference trials in an instructed-choice task and decision trials in a two-armed bandit decision task. We show that the activity of dopamine neurons in the decision setting is modulated according to the value of the upcoming action. Moreover, analysis of the probability matching strategy in the decision trials revealed that the dopamine population activity and not the reward during reference trials determines choice behavior. Because dopamine neurons do not have spatial or motor properties, we conclude that immediate decisions are likely to be generated elsewhere and conveyed to the dopamine neurons, which play a role in shaping long-term decision policy through dynamic modulation of the efficacy of basal ganglia synapses.**

The art of associating sensory information with appropriate behavior or decision making has been investigated through the prisms of a multitude of fields. The search for psychological<sup>1,2</sup> and neural correlates<sup>3–8</sup> of decision making was paralleled by machine learning research. One form of machine learning, reinforcement learning, has achieved popularity because of its efficiency and its resemblance to real-life situations. Developments in reinforcement learning have led to a powerful learning algorithm known as temporal difference (TD) learning<sup>9</sup>. TD learning, originally used for modeling classical conditioning, is based on evaluating sensory inputs, or states, by assigning them a value according to the anticipation of reward. Learning to optimize this evaluation is achieved by constant comparison of the value of the current state with its previous estimation. When a discrepancy arises, this difference, termed the TD error, is used to improve estimation of the state value.

The classical conditioning context provides an inadequate description of the typical reinforcement learning setting in which agents act upon sensory information to execute behavioral decisions. Moving from passive TD learning to active control requires modification of the computational algorithm, as the aim of learning has now shifted to optimization of actions in different states to maximize the long-term accumulated reward. The actions affect not only reward, but also the transition from one state to another, an outcome that must also be learned. This challenge is resolved by reinforcement learning models that incorporate actions into different variations of TD algorithms<sup>9,10</sup> using the TD error to update the state evaluation and to adjust the set of rules that govern the decisions in each state, or the policy.

Policy optimization can be achieved in a number of fashions. One way is through the design of specialized actor/critic network architecture. In these networks, the TD error is used to teach two

separate elements, which, when combined, result in efficient action selection. The critic estimates the values of all encountered states (as in the classical conditioning context), whereas the actor stores the policy and performs actions. Each action can lead to a different state. This may cause a deviation from the estimated value of the previous state. The resulting change, the TD error, is fed back to the actor by the critic and is used to shape the desired policy. An alternative class of algorithms does not involve explicit representation of the policy but relies on direct assessment of the value of state-action pairs (also termed action values or Q values) rather than the value of the state alone<sup>9–12</sup>. Thus, both the actor-critic and Q-value estimation models are taught by a TD error. This error signal is independent of the action in the actor-critic architecture, whereas a Q-value error signal is affected by the chosen action.

The phasic response of midbrain dopamine neurons located in the substantia nigra pars compacta (SNc) and the ventral tegmental area (VTA) is a likely neural correlate of the TD error, thus underscoring the applicability of the TD learning algorithm to neural learning<sup>8,13–18</sup>. Because the basal ganglia network, the main target of dopamine innervation, is commonly regarded as an action selection and generation system<sup>19,20</sup>, the dopamine signal is incorporated as the critique in actor/critic TD models of the basal ganglia<sup>19,21,22</sup>. In these models, the dopamine signal is used to reinforce behavior by adjusting synaptic efficacy in the appropriate neuronal circuits of the input layer of the basal ganglia networks—that is, the striatum<sup>23,24</sup>. Some models also use the dopamine signal to directly select possible actions<sup>24</sup>. Earlier electrophysiological recordings of dopamine neurons typically involved classical conditioning<sup>14,25</sup> or instructed-choice instrumental conditioning<sup>15–17</sup> tasks, but the role of dopamine in behavioral decisions involving competing actions and in policy formation has not been explored experimentally.

<sup>1</sup>Interdisciplinary Center for Neural Computation (ICNC), Hebrew University, Jerusalem, Israel. <sup>2</sup>Hebrew University, Department of Physiology, PO Box 12272, Jerusalem 91220, Israel. Correspondence should be addressed to G.M. (genela.morris@charite.de).

Received 27 March; accepted 28 June; published online 23 July 2006; doi:10.1038/nn1743

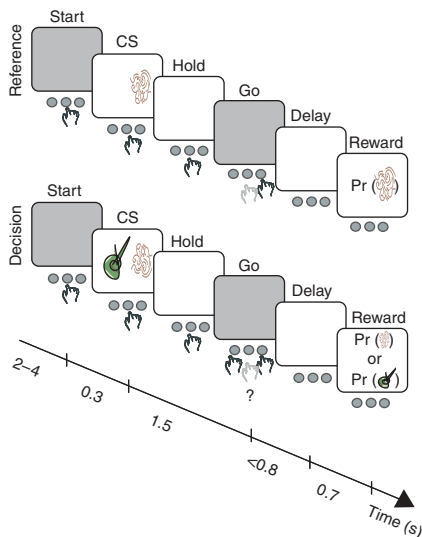


**Figure 1** Behavioral tasks and response parameters. Top, reference trials; screen display, desired action and duration of each stage are shown. Bottom, decision trials; same conventions as above. CS, conditioning stimulus.

To elucidate the role of SNc dopamine neurons in decision making, we recorded their activity in three monkeys performing trials of a two-armed bandit task (decision); these trials were randomly embedded in reference trials of a probabilistic instructed-choice task (reference) (Fig. 1, task details in Methods). Briefly, in reference trials (80–90% of all trials), monkeys were presented with one of four possible visual conditioned stimuli. The stimulus was a random geometrical shape occupying the right or left half of a computer screen. The location of the stimulus indicated the correct direction of the arm movement, and the stimulus identity indicated the probability of receiving a reward upon correct completion of the trial. In decision trials, monkeys were simultaneously presented with a pair of conditioned stimuli from the reference set, allowing them a choice of action and, consequently, a choice of reward probability. This behavioral setting therefore allowed us to map the TD error responses emitted by dopamine neurons in the reference task and to use them as a reference for the study of behavior in a decision

situation, as well as to study dopamine responses in the decision process itself.

## RESULTS

### Reference dopamine responses determine decision policy

We observed no differences in motor parameters (reaction time, movement time) between the two trial types (*t*-test,  $P > 0.2$ ). Thus it can be assumed that the monkeys used similar motor strategies and could use the information they gathered in the reference trials to determine their behavior in the decision context. Two related parameters in the reference trials could impact the decision policy: the delivered reward and the TD error–like dopamine activity in these trials. We examined the monkeys' choices in the decision trials ( $C$ ), and their relation to the reward rate ( $R$ ) and dopamine responses to the conditioning stimuli ( $D$ ) in the reference trials (Fig. 2). Because dopamine activity was highly correlated with reward rate ( $R^2 = 0.918$ ), the policy-determining factor could be the reward rate itself or the dopamine activity. In one model (Fig. 2b, inset), decision choices are governed by the reference reward rates, which independently also modulate the reference dopamine activity. In the alternative model (Fig. 2d, inset), the impact of reference reward on decision choices is mediated by the reference dopamine activity.

Reference reward rates (Fig. 2a) were computed as the *a priori* reward probability corrected by the monkeys' error rates on those trials. In the reference task, the reward-choice relationship was monotonic (Fig. 2b). The monkeys' policy was thus a suboptimal probability matching strategy<sup>26,27</sup> ( $R^2 = 0.884$ ,  $P < 0.001$ ):

$$C_{\text{right}} \propto \frac{R_{\text{right}}}{R_{\text{right}} + R_{\text{left}}},$$

where  $C$  is the probability of a particular choice and  $R$  is the probability of being rewarded on that choice. Logistic regression analysis, which should be applied to relations between a proportion and a continuous variable, yielded a highly significant relation (likelihood ratio test,  $P < 0.001$ ).

Comparable studies in human subjects report a similar monotonic relationship in inexperienced gamblers, in contrast to trained gamblers who tend to maximize their return<sup>27</sup>. Our design, in which decision trials were only sparsely embedded in the reference trials, is a primate model for this situation. Recent studies in repeated decision tasks<sup>4,28</sup> show local dependence of choice behavior on reward history. Our task

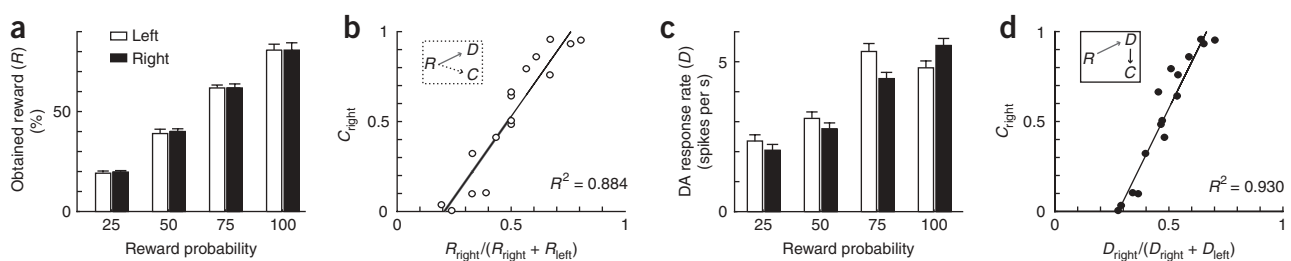


**Figure 2** Contribution to probability matching behavior. (a) The probability of being rewarded after presentation of each conditioned stimulus in reference trials, corrected for errors in which the monkeys pressed the wrong key. Bars reflect mean, error bars are s.e.m. (b) Probability of choosing an alternative in the decision trials as a function of the relative probability of being rewarded for that alternative in the reference trials, computed from a. For visibility, the independent variable is displayed on a linear scale, although the  $R^2$ -value was computed using angular transformation (Methods). The 16 points represent all combinations of pairs of the four visual stimuli. Inset, possible interactions between reward ( $R$ ), dopamine signal ( $D$ ) and choices ( $C$ ); probability of reward has a dual effect: inducing activity in dopamine neurons and determining the monkeys' choices. (c) Dopamine reinforcement signal ( $D$ ), computed as the deviation from baseline firing rate following the conditioned stimuli in the reference trials. Bars reflect mean, error bars are s.e.m.  $n = 97$  neurons, data averaged across trials. (d) Probability of choosing an alternative in the decision trials as a function of the relative dopamine response to that alternative in the reference trials, computed from c. Conventions and scales as in b. Inset, the effect of reward on choices is mediated by the reinforcing dopamine signal. DA, dopamine.

design precludes such a behavioral strategy and indeed, choice-triggered analysis did not reveal any local history effects (Supplementary Fig. 1 online).

We studied the monkeys' decision behavior as predicted by the relative dopamine population reinforcement signal in the reference trials (Fig. 2c,d). Dopamine population responses were quantified as the difference in firing rate between the baseline activity and the responses to the visual conditioned stimuli (Fig. 2c). These responses were used to predict choice behavior in the decision task (Fig. 2d). The highly significant linear correlation between reference dopamine and decision choice behavior ( $R^2 = 0.930$ ) was corroborated by logistic regression analysis (likelihood ratio test,  $P < 0.001$ ). Moreover, the logistic fit of choice behavior to dopamine activity was significantly better than the fit to reward rate (likelihood ratio test,  $P < 0.05$ ). To examine the interplay between the three variables  $R$ ,  $D$  and  $C$ , we conducted a logistic regression analysis on the full model. In this analysis, decision choice behavior is described in terms of the contributions of both the reference reward rates and reference dopamine activity. The full model contained only one significant predictor, dopamine activity ( $P < 0.05$ ); reward rate was not a significant factor ( $P > 0.3$ ). Thus, the correlation between choices and dopamine reinforcement is not a byproduct of the common dependence on reward rate in the reference task. Rather, the reference dopamine response can be viewed as the mediator between reward and choice behavior. Partial correlation analysis yielded similar results (Supplementary Note online).

### Decision choices are not predicted by early gaze shifts

Before examining dopamine activity during decision trials, we must rule out possible confounding effects of different gaze positions before and during the neuronal response. We compared the horizontal eye positions recorded during the later part of the 'start' period with those during the conditioned stimulus presentation (Fig. 1). We separated, according to future action, all traces of the horizontal axis of eye positions recorded during reference and decision trials (Fig. 3a). In this example session, the eye positions in the reference trials at the time of stimulus presentation (onset indicated by arrowhead) differed slightly according to stimulus position (and, consequently, according to the direction of the future arm movement), but in decision trials, the eye positions were similar regardless of future movement.

To quantify possible differences in the visual inputs to the monkeys (and to SNc dopamine neurons<sup>29</sup>), which may have affected the neuronal results, we first examined differences in gaze direction in the decision trials for trials in which opposing actions were taken. A two-tailed  $t$ -test between the groups of eye positions at two time points—the time of stimulus presentation and 400 ms after presentation (neuronal responses were examined in this 400-ms window)—indicated no differences ( $P > 0.3$  in all recorded sessions). We further examined the gaze positions by principal component analysis (PCA; Methods) by taking the 1 s preceding and the 400 ms following the visual stimulus presentation (green line in Fig. 3a) and projecting all traces on the space defined by the first and second principal components (Fig. 3b, left) and by the third and fourth components (right). In

this example, the first four components explain 77.4% of the variability. In the reference task, the two movement directions were reflected in the gaze positions, but the projections of the eye movements in the decision tasks overlapped, indicating that they did not depend on future movement. We repeated this analysis on all recording sessions. In all cases, the first four components accounted for  $>70\%$  of the variability. In no session were the decision trials separable based on future movement. As expected, the separation between clusters in the period surrounding the 'go' signal was far better both in reference and decision trials. Finally, for each decision

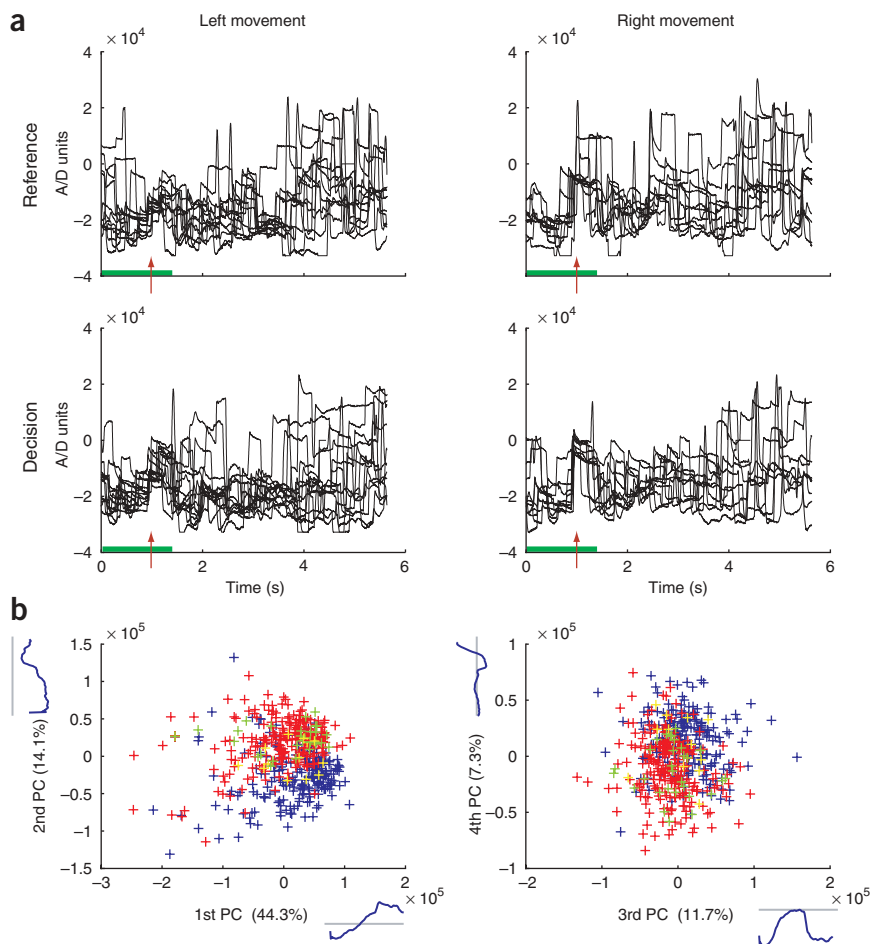


**Figure 3** Eye positions in reference and decision trials. (a) Example traces of horizontal eye position from an entire recording session recorded from monkey C. Left, all traces surrounding presentation of conditioned stimuli (arrowhead) that were followed by 'left' movement in reference (top) and decision (bottom) trials. Right, all traces surrounding presentation of conditioned stimuli (arrowhead) that were followed by 'right' movement in reference (top) and decision (bottom) trials. (b) Example of principal component analysis (PCA). All segments between 1 s before and 400 ms after stimulus presentation of the example shown in a (green bars) are projected on the first two principal components (PCs) (left) and the third and fourth principal components (right). The principal components and the fraction of variability they account for are indicated along the axes. Key: red +, reference right; blue +, reference left; green +, decision right; yellow +, decision left.

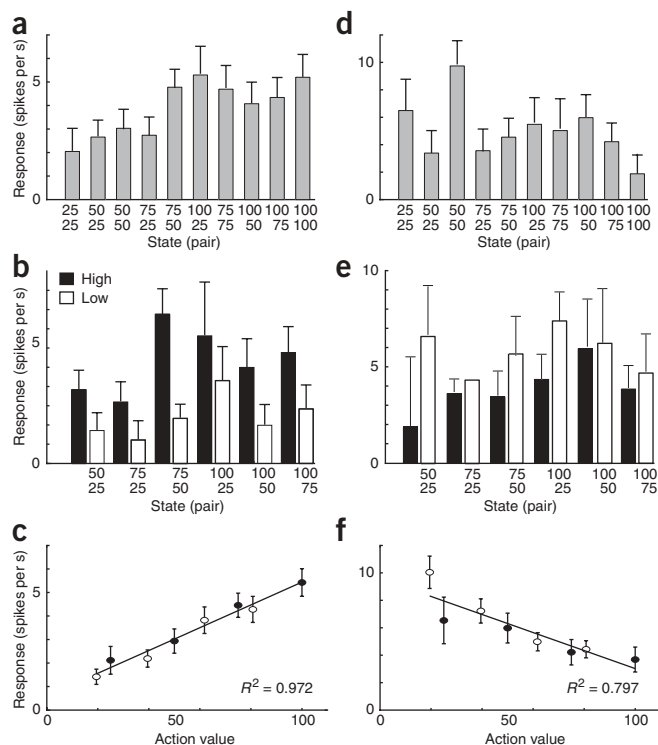


**Figure 4** Dopamine neurons code the TD error of action value. **(a)** Dopamine responses to pairs of conditioned stimuli in decision trials, presented in ascending order according to state value (defined as the average probability of reward following each pair). Bars reflect mean, error bars are s.e.m. ( $n = 97$  neurons). **(b)** Dopamine responses to pairs of conditioned stimuli in decision trials, separated according to the chosen action. Bars reflect mean, error bars are s.e.m. ( $n = 97$  neurons). **(c)** Dopamine responses to conditioned stimulus in reference (empty circles) and decision (filled circles) trials, as a function of the action value (defined as the average probability of reward following each action). In the reference trials, the expected reward probability is corrected for response errors. By definition, there are no response errors in the decision trials. Points reflect mean  $\pm$  s.e.m. ( $n = 97$  neurons). **(d-f)** Dopamine responses to reward delivery in the rewarded decision trials. All conventions are as in **a-c**.

decision trials depended on the monkeys' choice of future action. We therefore separated the decision trials based on the action taken at the completion of the trials. When the mean population responses to the presentation of six pairs of nonidentical stimuli were separated according to choice of future action, in all pairs the dopamine signal was significantly higher when the monkeys chose the key associated with the higher probability of reward (*post-hoc* comparison,  $P < 0.01$ ; **Fig. 4b**).

To uncover the effects underlying this variability, a two-way ANOVA was applied to the data. This analysis showed a clear main effect of chosen cue ( $P < 0.001$ ), with no effect of the discarded cue ( $P > 0.4$ ), and a marginal interaction effect ( $P = 0.05$ ), resulting from the difference in dopamine responses when the 75% cue was chosen. We therefore pooled the data of the dopamine responses to the conditioned stimulus in the decision trials according to the value of the chosen actions (**Fig. 4c**, solid circles). Response of the dopamine neurons to the conditioned stimuli differed significantly according to future actions (one-way ANOVA,  $P < 0.001$ ). Furthermore, the responses were proportional to the theoretical value of the different actions, similarly to the differential responses in the reference trials<sup>16</sup>.

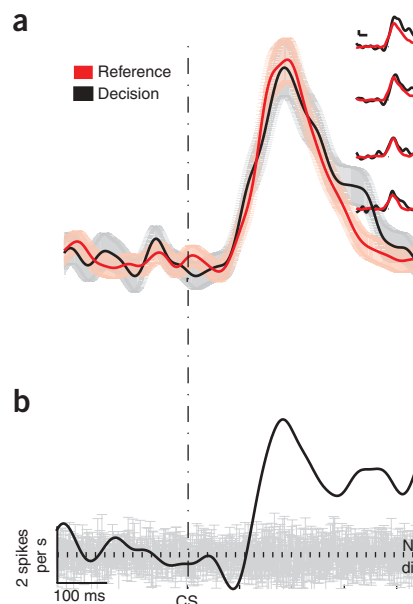
This finding points to a new interpretation of the dopamine responses observed in previous classical conditioning and instructed-choice experiments. Under these conditions, action is trivial or non-existent and therefore does not alter the neuronal responses. To

trial, we calculated an index indicating the relative time the monkey gazed to the right during the 1.4-s period described above. The  $z$ -transformation of this index (Methods) in left-movement trials was compared to that in right-movement trials by  $t$ -test. In all examined days, no difference was found between right- and left-movement decisions ( $P > 0.2$  in all sessions).

### Decision dopamine responses reflect future action

The monkeys' probability matching policy, which exhibited a variability of responses in identical situations, allowed us to explore dopamine neuron activity during decision making. The activity of different neurons was pooled to analyze the dopamine population response. The dopamine response in the reference trials accurately represents the TD error in the estimation of the state value—that is, the average expected reward<sup>14,16</sup>. On the other hand, in decision trials responses of the population of dopamine neurons to each of the decision stimulus pairs were ranked according to their state value, these responses were statistically indistinguishable ( $P > 0.1$ , one-way analysis of variance (ANOVA); **Fig. 4a**). However, in contrast to the instructed-choice reference trials, the prospects of reward in the

**Figure 5** Time course of the responses of dopamine neurons in the reference and decision tasks. **(a)** Evolution in time of the population responses to the conditioned stimulus in reference (red) and decision (black) trials. The response (baseline subtracted) was averaged for all conditioned stimuli, pooled together and smoothed with a Gaussian filter (s.d. = 10 ms). The shading indicates the s.e.m. of the average responses. Inset, average responses to the stimulus in reference and decision trials, separated according to their action values (in descending order). **(b)** The time course of differential activation between the pairs of choices made in the decision trials. Population averaging and smoothing as in **a**. Gray bars indicate the 95% confidence interval in the theoretical situation where there are no differential responses, calculated using a randomization procedure of all choices ( $n = 1,000$ ). Dotted line indicates zero. Dashed vertical line indicates the time of stimulus presentation. Time and firing scale are common for **a** and **b**.





illustrate the full dependence of the dopamine response on the expected reward probability given the chosen action (that is, the state-action value), we combined the results from the reference (empty circles) and decision trials (linear regression,  $R^2 = 0.972$ ; Fig. 4c). To examine the consistency of the dopamine responses with the TD error signal associated with the action value (Q value), we analyzed the complementary dopamine responses to received reward in the decision trials (Fig. 4d–f). As predicted, the dependence of dopamine responses on the action value was reversed (but see Methods for statistical limits of this analysis). The responses of all neurons are consistent with this picture (Supplementary Fig. 2 online).

Finally, we examined the time course of development of choice-related activity in the dopamine neurons (Fig. 5). The similarity of the time course of neuronal activation in the decision and reference trials (Fig. 5a) challenges the attractive notion that dopamine neurons code the action value in two stages, the first relating to the state value and the second adjusting for the action value. Choice-related activity was defined as the time course of differential activation in response to the high- versus low-probability cue choices in the decision task (Fig. 5b). The differential response crossed the upper limit of the 95% confidence interval 122 ms after stimulus presentation. This time course is very similar to the development of information regarding the state value in reference conditions<sup>16</sup>. Therefore, although this differentiation may serve as an indication of the upper bound on the time of decision formation, it cannot provide us with further insight into the dynamics of the decision process.

## DISCUSSION

The results presented in this report provide key insight into the role of dopamine in decisions, both in the long-term modification of behavior and in immediate decision making. First, probability matching decision behavior is likely to be mediated by the activity of dopamine neurons rather than by reward in the reference trials, suggesting that the history of dopamine responses shapes long-term behavioral policy. Second, the activity of dopamine neurons reflects future choice of action as early as 122 ms after the presentation of the conditioning stimulus. This has implications for the position of dopamine in the hierarchy of decision making: that is, it is likely that dopamine neurons receive information about the decision from another structure. Both these results jibe with claims in previous lesion and behavioral studies regarding the long-term rather than immediate effect of dopamine on reward-oriented behavior<sup>30</sup>.

An alternative conclusion would be that the signal of the dopamine neurons reports the error for the state value and that it directly determines decision. Some models have adopted this view<sup>24</sup>, in which the TD state value signal has an additional effect on the probability of an upcoming action. However, because the dopamine signal is extremely homogenous in the origin structures<sup>13</sup> and highly widespread at the targets<sup>31,32</sup>, the possibility of separate TD signals for each alternative can be excluded. Therefore, such models of the direct effect of dopamine on immediate decisions can only apply to situations involving evaluation of a single alternative. In our decision setup, as in many real-life situations, this is not the case. Therefore, if the dopamine signal is used for immediate decision, the multiple choices must be translated into a single choice. For example, the deciding circuits may use the dopamine TD signal to determine the probability of the action that maximizes reward expectation. However, this strategy will collapse in scenarios where there are multiple ( $> 2$ ) choices.

We therefore favor the complementary hypothesis, that dopamine neurons are already informed of an upcoming action. The striatal projection neurons could follow a probabilistic policy<sup>7</sup>, which is shaped

by the history of dopamine reinforcement. Two broad classes of reinforcement learning models, incorporating an action-generation mechanism into different variations of TD algorithms<sup>9</sup>, were proposed to accommodate for decision making. In the actor/critic model, the network includes a separate policy-performing element, the actor, as well as a reward-predicting element, the critic. In the other model, the behavior is integrated into the evaluation process, assigning a separate value (Q value) to each possible behavioral choice in every state. Most reinforcement learning models of the basal ganglia adopt the actor/critic view and thus stress the importance of learning state values. This model was supported by single-unit recordings of dopamine neurons<sup>33</sup> and by other studies<sup>31</sup> using classical conditioning and instructed-choice designs, but has never been tested in decision contexts. Our results call for a reappraisal of the current computational models of dopamine and the basal ganglia so that they incorporate the learning and estimation of Q values (as achieved by the SARSA learning algorithm<sup>9</sup> or advantage learning<sup>12</sup>) into the learning and decision algorithms of these neuronal structures.

## METHODS

**Animal training and behavioral tasks.** Data were obtained from three macaque monkeys (*Macaca fascicularis*, two females, monkeys C and E; one male, monkey Y), weighing 2.5–4 kg. Care and surgical procedures were in accordance with the US National Institutes of Health Guide for the Care and Use of Laboratory Animals (1996) and with Hebrew University guidelines for the use and care of laboratory animals in research, supervised by the institutional animal care and use committee.

The monkeys were trained on a task with randomly ordered, intermittent, instructed-choice, instrumental conditioning trials (reference, 80%–90% of trials) and two-armed bandit decision trials (decision, 10%–20% of trials) (Fig. 1). In all trials, the monkeys faced a 17" computer screen placed at a distance of approximately 40 cm. A panel with three keys was located at arm's length. Trials were initiated when the monkey touched the central key. After a variable delay (1.5–2.5 s in monkeys C and E, 2–4 s in monkey Y), the visual conditioned stimulus appeared for a short period (0.3 s for monkeys C and E, 0.45 s in monkey Y).

In reference trials, the conditioned stimulus, located either on the left or the right side of the screen, was one of a set of four, each associated with a different probability (0.25, 0.50, 0.75 and 1.00) of receiving an equal amount of reward upon correct trial completion. The visual stimulus occupied half of the screen (corresponding to approximately  $24 \times 36$  visual degrees). The stimulus presentation was followed by a fixed hold period (2 s for monkeys Y and C, 1.5 s for monkey E), after which a 'go' signal appeared. The monkeys were required to press either the left or the right key, corresponding to the location of the memorized stimulus, within an allowed response time of 800 ms for monkeys C and E and 700 ms for monkey Y. Correct responses were followed (with an interval of 700 ms) by a liquid reward, according to the probability associated with the conditioned stimulus. No external stimulus indicated the expected time of the reward.

In decision trials, the stimulus presentation phase consisted of a simultaneous display of two stimuli in both possible locations, and the monkeys could choose to press either the left or the right key. Equal-probability stimulus pairs were not excluded. The monkeys were then rewarded according to the probability associated with the stimulus that appeared in the chosen location. All other parameters (prestimulus duration, stimulus duration, hold duration, maximum response time and reward delay) were identical in the decision and reference trials.

All trials (incorrect, correct, rewarded and unrewarded) were followed by a variable intertrial interval (ITI): 3–6 s in monkeys E and C, 5–7 s in monkey Y. The monkeys performed 300–500 trials on most training and recording days. Monkeys were trained for 5–6 d per week and were allowed free access to food and water on the weekends. The monkeys were not trained for gaze fixation.

The trial sequence was completely randomized. Every trial was chosen, with a preset probability, to be either a reference trial ( $P = 0.8$  or  $0.9$ ) or a decision trial ( $P = 0.1$  or  $0.2$ ). In reference trials, the right or left locations of the

stimulus were then drawn with an equal probability, as was the stimulus identity. In decision trials, the stimuli on each side were chosen in the same way. All trial parameters (trial type, stimulus location and identity and the length of the variable-duration trial segments) were randomly chosen with the same random number generator. To avoid repetition of the same random sequence, the seed of the random number generator was changed with each initiation of the behavioral program, based on absolute time (srand and rand functions, Visual C++ 6.0).

The monkeys were fully trained on the task and acquainted with all possible stimuli before the recording chamber was implanted. Training consisted of familiarization with the behavioral setup (12–20 training days), followed by training on the task in a deterministic regime in which all correctly performed trials were rewarded (60–92 training days, to a criterion of 80% correct performance). For this part of the training we used a different stimulus from those used in the experiment. Finally, we introduced the set of conditioned stimuli and the associated reward probabilities (for 30–41 training days). The same set was then used in the recording days (45–150 days of recording from multiple structures).

**Magnetic resonance imaging (MRI) localization of recording targets.** We estimated the stereotaxic coordinates of the substantia nigra pars compacta (SNc) according to MRI scans aligned with an anatomical atlas of *Macaca fascicularis*<sup>34,35</sup>. After training, a square Cilux recording chamber with a 27-mm (inner) side was attached to the skull with its center targeted at stereotaxic coordinates of the SNc. The recording chamber was tilted 40–50° laterally in the coronal plane. The chamber's coordinate system was adjusted according to MRI imaging. An MRI scan (Biospec Bruker 4.7 Tesla animal system, fast-spin echo sequence; effective TE = 80 ms and TR = 2.5 s; 13 coronal slices, 1 or 2 mm wide) was performed with 150- $\mu$ m diameter tungsten electrodes at accurate coordinates of the chamber. We then aligned the two-dimensional MRI images with the sections of the atlas. All surgical and MRI procedures were performed under general and deep anesthesia.

**Recording and data acquisition.** During recording sessions, the monkeys' heads were immobilized, and 4–8 glass-coated tungsten microelectrodes (impedance 0.3–1.2 M $\Omega$  at 1,000 Hz), confined within a cylindrical guide (1.65 mm inner diameter), were advanced separately (EPS, Alpha-Omega Engineering) into the SNc. The electrical activity was amplified with a gain of  $\times 10$ k and band-pass filtered with a 300–6,000 Hz four-pole Butterworth filter (MCP+, Alpha-Omega Engineering). Upon reaching the target area in the SNc, as judged by the stereotaxic and MRI coordinates and by the electrophysiological hallmarks of the encountered structures along the penetration, dopamine cells were identified according to their low frequency (<15 Hz nonperiodic discharge), long duration (>1.5 ms) and polyphasic spikes<sup>36,37</sup>, and by a firing elevation in background single- and multi-unit activity in response to unexpected reward<sup>34,38</sup>. After recording, the electrode tracks were generally followed to the neighboring structures, further aiding verification of the recorded structures<sup>39</sup>.

Neuronal activity was sorted and classified online using a template-matching algorithm (MSD, Alpha-Omega Engineering). Spike-detection pulses and behavioral events were sampled at 12 kHz (AlphaMap, Alpha-Omega Engineering). Gaze positions were recorded by an infrared reflection detector (Dr. Bouis). The infrared signal was amplified with a gain of  $\times 500$ , band-pass filtered with a 1–100 Hz four-pole Butterworth filter (MCP+, Alpha-Omega Engineering), and sampled at 750 Hz. The signal was not calibrated and thus did not allow for conversion of analog to digital (A/D) units to visual angles. In addition, three digital video cameras recorded the monkeys' faces and upper and lower limbs.

**Statistical analysis.** The first step in the neuronal data analysis targeted verification of the real-time isolation quality and stability of the spiking activity. Only spike trains considered to be emitted by a single cell during real-time sorting were subjected to rate-stability analysis, in which the instantaneous firing rate of the neuron in task-neutral periods was examined for changes. The firing rate during the ITI period in consecutive trials in the entire recording session was graphically displayed, and the largest continuous segment of stable data was selected for further analysis. Stable cells were chosen for the database after examination for response to at least one behavioral event (visual stimulus, reward, and reward-omission) in the reference task, using a

Mann-Whitney *U*-test ( $P < 0.05$  after a Bonferroni correction for multiple comparisons). Only cells that were stable for at least five trials of each condition in the reference task and at least three pair combinations in the decision task were included.

Cell responses to behavioral events for ANOVA, linear regression, logistic regression and partial correlation analysis were parameterized as the difference between average firing rate in the 400 ms following the event and that in the preceding 400 ms. The 400-ms time window was chosen as the average time in which neuronal responses in reference trials returned to baseline (Fig. 5). Some individual neurons had longer responses. We therefore repeated the analyses with 500-ms windows. This analysis yielded comparable results. The neuronal data presented here relies on population averages of all recorded cells, normalized by the number of trials recorded from each cell. Averaging responses normalized for baseline firing rate, as well as for maximum response rate, did not affect the results.

For linear regression of the relative fraction of choice as a function of the relative neuronal and reward reinforcements, the proportion variables ( $p$ ) were converted from the [0,1] range using an angular transformation<sup>40</sup>:  $\theta = \arcsin(\sqrt{p})$ .

Choice probability was also examined using logistic regression analysis<sup>40</sup>, which investigates the relation of continuous independent variables to binomial dependent variables by the following logistic model:

$$p = \frac{e^{\beta^T x}}{1 + e^{\beta^T x}},$$

where  $p$  is the probability of the dependent variable,  $x$  is the vector of predictors and  $\beta$  is a vector of the regression coefficients. The parameters of the logistic model were estimated using maximum likelihood estimation, and the overall likelihood of the model can be examined and compared to other models.

Statistical analysis of the neuronal data during reward delivery in decision trials is problematic, owing to the experimental design and the behavioral strategy of the monkeys. Because of the probabilistic regime of our reward schedule, the number of rewards increased consistently with the presumed independent variable, the 'action value', creating an imbalance in the respective sample sizes and their variability. This effect was also inflated by the monkeys' probability matching behavior (Fig. 2b).

Traces of eye position recordings were subjected to three statistical tests to verify that future action in decision trials was not correlated with eye positions in early segments of the trial. A *t*-test checked for systematic differences in gaze direction between trial types at the time of the stimulus presentation and at the end of the examination window of neuronal responses (400 ms after cue onset). To identify possible temporal patterns of eye movement, PCA was conducted on all sequences of sampled eye positions; the analyzed segments started 1 s before the stimulus display and ended 400 ms after display, at which time our examination of neuronal responses ended. In this type of analysis, the multi-dimensional data are searched for a smaller set of dimensions that define a new space that explains most of the variability in the data. These dimensions or principal components are ordered according to the fraction of variability for which they account. Formally, the principal components are the eigenvectors of the covariance matrix describing the data. One application of PCA is clustering of data by projecting the different data points onto the lower dimension space. We projected the eye positions from the reference trials in the relevant 1,400-ms trial segment onto the two-dimensional spaces defined by the first and second components and by the third and fourth components (Fig. 3b), to search for visually distinguishable clusters between the two movement directions (right and left). We then added the data points corresponding to the decision trials and visually examined their mapping in these spaces. Finally, we devised an index indicating the amount of time the gaze was directed toward the right during segments starting 1 s before stimulus display and ending 400 ms after display. We established the baseline as the mean horizontal eye position during the ITI. Variability was assessed in the same period. 'Right' annotates all samples in which the A/D value exceeded baseline by over 1 s.d., and 'left' annotates the samples below baseline by at least 1 s.d. (more conservative thresholds were also checked, yielding qualitatively similar results):

$$See_{\text{right}} = \frac{T_{\text{right}} - T_{\text{left}}}{T_{\text{trial}}},$$

where  $T_{\text{right}}$  is the number of samples gazing right in a trial.

To transform this index into a normally distributed variable we computed its Fisher  $z$ -transformation<sup>40</sup>:

$$Z_{\text{right}} = \frac{1}{2} \ln \left( \frac{1 + \text{See}_{\text{right}}}{1 - \text{See}_{\text{right}}} \right)$$

and subjected this new variable to a  $t$ -test.

All data analysis was performed using Matlab 7.0 (MathWorks) code.

Note: Supplementary information is available on the Nature Neuroscience website.

#### ACKNOWLEDGMENTS

We thank Y. Prut, Y. Engel, Y. Ritov, N. Daw, Y. Niv and R. Paz for fruitful discussions and comments on earlier versions of this manuscript; and G. Goelman and V. Sharkansky for technical assistance. This study was partly supported by a Center of Excellence grant administered by the Israel Science Foundation (ISF) and by a 'Fighting against Parkinson' grant administered by the Netherlands Friends of the Hebrew University (HUNA). G.M. was supported by a Horowitz fellowship.

#### COMPETING INTERESTS STATEMENT

The authors declare that they have no competing financial interests.

Published online at <http://www.nature.com/natureneuroscience>

Reprints and permissions information is available online at <http://npg.nature.com/reprintsandpermissions/>

- Herrnstein, R.J. On the law of effect. *J. Exp. Anal. Behav.* **13**, 243–266 (1970).
- Tversky, A. & Kahneman, D. The framing of decisions and the psychology of choice. *Science* **211**, 453–458 (1981).
- Bayer, H.M. & Glimcher, P.W. Midbrain dopamine neurons encode a quantitative reward prediction error signal. *Neuron* **47**, 129–141 (2005).
- Sugrue, L.P., Corrado, G.S. & Newsome, W.T. Matching behavior and the representation of value in the parietal cortex. *Science* **304**, 1782–1787 (2004).
- Romo, R., Hernandez, A. & Zainos, A. Neuronal correlates of a perceptual decision in ventral premotor cortex. *Neuron* **41**, 165–173 (2004).
- Barracough, D.J., Conroy, M.L. & Lee, D. Prefrontal cortex and decision making in a mixed-strategy game. *Nat. Neurosci.* **7**, 404–410 (2004).
- Samejima, K., Ueda, Y., Doya, K. & Kimura, M. Representation of action-specific reward values in the striatum. *Science* **310**, 1337–1340 (2005).
- Pagnoni, G., Zink, C.F., Montague, P.R. & Berns, G.S. Activity in human ventral striatum locked to errors of reward prediction. *Nat. Neurosci.* **5**, 97–98 (2002).
- Sutton, R.S. & Barto, A.G. *Reinforcement Learning: an Introduction* (MIT Press, Cambridge, Massachusetts, 1998).
- Rummery, G.A. & Niranjan, M. On-line Q-learning using connectionist systems. *Technical Report CUED/F-INFENG/TR 166* (Engineering Department, Cambridge University, Cambridge, UK, 1994).
- Watkins, C.J.C.H. & Dayan, P. Q learning. *Mach. Learn.* **8**, 279–292 (1992).
- Dayan, P. & Balleine, B.W. Reward, motivation, and reinforcement learning. *Neuron* **36**, 285–298 (2002).
- Schultz, W., Dayan, P. & Montague, P.R. A neural substrate of prediction and reward. *Science* **275**, 1593–1599 (1997).
- Fiorillo, C.D., Tobler, P.N. & Schultz, W. Discrete coding of reward probability and uncertainty by dopamine neurons. *Science* **299**, 1898–1902 (2003).
- Satoh, T., Nakai, S., Sato, T. & Kimura, M. Correlated coding of motivation and outcome of decision by dopamine neurons. *J. Neurosci.* **23**, 9913–9923 (2003).
- Morris, G., Arkadir, D., Nevet, A., Vaadia, E. & Bergman, H. Coincident but distinct messages of midbrain dopamine and striatal tonically active neurons. *Neuron* **43**, 133–143 (2004).
- Nakahara, H., Itoh, H., Kawagoe, R., Takikawa, Y. & Hikosaka, O. Dopamine neurons can represent context-dependent prediction error. *Neuron* **41**, 269–280 (2004).
- Pan, W.X., Schmidt, R., Wickens, J.R. & Hyland, B.I. Dopamine cells respond to predicted events during classical conditioning: evidence for eligibility traces in the reward-learning network. *J. Neurosci.* **25**, 6235–6242 (2005).
- Gurney, K., Prescott, T.J., Wickens, J.R. & Redgrave, P. Computational models of the basal ganglia: from robots to membranes. *Trends Neurosci.* **27**, 453–459 (2004).
- Mink, J.W. The basal ganglia: focused selection and inhibition of competing motor programs. *Prog. Neurobiol.* **50**, 381–425 (1996).
- Bar-Gad, I., Morris, G. & Bergman, H. Information processing, dimensionality reduction and reinforcement learning in the basal ganglia. *Prog. Neurobiol.* **71**, 439–473 (2003).
- Barto, A.G. Adaptive critics and the basal ganglia. in *Models of Information Processing in the Basal Ganglia* (eds. Houk, J.C., Davis, J.L. & Beiser, D.G.) 215–232 (MIT Press, Cambridge, Massachusetts, 1995).
- Reynolds, J.N., Hyland, B.I. & Wickens, J.R. A cellular mechanism of reward-related learning. *Nature* **413**, 67–70 (2001).
- McClure, S.M., Daw, N.D. & Montague, P.R. A computational substrate for incentive salience. *Trends Neurosci.* **26**, 423–428 (2003).
- Tobler, P.N., Fiorillo, C.D. & Schultz, W. Adaptive coding of reward value by dopamine neurons. *Science* **307**, 1642–1645 (2005).
- Wolford, G., Miller, M.B. & Gazzaniga, M. The left hemisphere's role in hypothesis formation. *J. Neurosci.* **20**, RC64 (2000).
- Vulkan, N. An economist's perspective on probability matching. *J. Econ. Surv.* **14**, 101–118 (2000).
- Lau, B. & Glimcher, P.W. Dynamic response-by-response models of matching behavior in rhesus monkeys. *J. Exp. Anal. Behav.* **84**, 555–579 (2005).
- Dommett, E. *et al.* How visual stimuli activate dopaminergic neurons at short latency. *Science* **307**, 1476–1479 (2005).
- Wise, R.A. Dopamine, learning and motivation. *Nat. Rev. Neurosci.* **5**, 483–494 (2004).
- Cragg, S.J. & Rice, M.E. DANCing past the DAT at a DA synapse. *Trends Neurosci.* **27**, 270–277 (2004).
- Wickens, J.R. & Arbutnot, G.W. Structural and functional interactions in the striatum at the receptor level. in *Dopamine* (eds. Dunnett, S.B., Bentivoglio, M., Bjorklund, A. & Hokfelt, T.) 199–236 (Elsevier, Amsterdam, 2005).
- Waelti, P., Dickinson, A. & Schultz, W. Dopamine responses comply with basic assumptions of formal learning theory. *Nature* **412**, 43–48 (2001).
- Szabo, J. & Cowan, W.M. A stereotaxic atlas of the brain of the cynomolgus monkey (*Macaca fascicularis*). *J. Comp. Neurol.* **222**, 265–300 (1984).
- Martin, R.F. & Bowden, D.M. *Primate Brain Maps: Structure of the Macaque Brain* (Elsevier Science, Amsterdam, 2000).
- Grace, A.A. & Bunney, B.S. Intracellular and extracellular electrophysiology of nigral dopaminergic neurons-1. Identification and characterization. *Neuroscience* **10**, 301–315 (1983).
- Ungless, M.A., Magill, P.J. & Bolam, J.P. Uniform inhibition of dopamine neurons in the ventral tegmental area by aversive stimuli. *Science* **303**, 2040–2042 (2004).
- Hollerman, J.R. & Schultz, W. Dopamine neurons report an error in the temporal prediction of reward during learning. *Nat. Neurosci.* **1**, 304–309 (1998).
- Nevet, A., Morris, G., Saban, G., Feinstein, N. & Bergman, H. Discharge rate of substantia nigra pars reticulata neurons is reduced in non-parkinsonian monkeys with apomorphine-induced orofacial dyskinesia. *J. Neurophysiol.* **92**, 1973–1981 (2004).
- Sokal, R.R. & Rohlf, F.J. *Biometry* (W.H. Freeman & Co., New York, 1981).